Q-space and Conventional DWI of Axonal and Myelin Damage in the Rat Spinal Cord after Axotomy

J. A. Farrell[1,2], J. Zhang[2], M. Jones[3], C. A. DeBoy[3], P. N. Hoffman[3,4], S. A. Smith[1,2], D. S. Reich[3,5], P. A. Calabresi[3], and P. C. van Zijl[1,2]

[1]F.M. Kirby Research Center for Functional Brain Imaging, Kennedy Krieger Institute, Baltimore, Maryland, United States, [2]Neuroscience Section, Division of MR Research, Dept. of Radiology, Johns Hopkins University School of Medicine, Baltimore, Maryland, United States, [3]Dept. of Neurology, Johns Hopkins University School of Medicine, Baltimore, Maryland, United States, [4]Dept. of Ophthalmology, Johns Hopkins University School of Medicine, Baltimore, Maryland, United States, [5]Division of Neuroradiology, Dept. of Radiology, Johns Hopkins University School of Medicine, Baltimore, Maryland, United States

Introduction: Axonal and myelin damage are common in multiple sclerosis. While diffusion weighted MRI (DWI) has shown great potential, the relationships between degenerating white matter (WM) microstructure and DWI signal intensity are still a topic of investigation. In this study, we investigate diffusion perpendicular and parallel to the rat spinal cord after dorsal root axotomy. This model results in rapid axonal degeneration followed by delayed myelin damage in the dorsal column [1]. Unlike conventional DWI analysis, q-space analysis estimates the probability density function (PDF) for diffusion without the need to assume a Gaussian shape [2,3]. Q-space analysis is well suited to study diffusion in WM fibers and has been applied to myelin development [4], myelin deficiency [5], and crush injury [6] in the rat spinal cord. With the goal of determining which diffusion contrasts are specific to axonal and myelin damage, we compare q-space contrasts to conventional anisotropy and diffusivity measurements at low b-values and to histology.

Methods: Six Lewis rats were anesthetized and the left L2-4 dorsal roots were transected rostral to ganglion, thereby affecting ascending fibers in the dorsal column. Three and 30 days after injury (N = 3 each), rats were anaesthetized and perfused with PBS followed by 4% PFA. The spinal cord was excised, fixed overnight at 4 °C, and stored in PBS. Data were acquired on an 11.7T Bruker spectrometer (5-mm saddle coil) using a stimulated echo (TR/TE/δ/Δ, = 1600/18.5/3/81 ms) with 5 axial slices covering T10 to L1 (0.1x0.1x1.5 mm). Diffusion weighted images (DWIs) were acquired at 12 q-values ($q = \gamma\delta G/2\pi$) from 102 to 1533 cm^{-1} (b_{max}= 74202 s/mm^2), and 8 q-values from 102 to 575 cm^{-1} (b_{max}= 10435 s/mm^2) for diffusion weighting perpendicular and parallel to the spinal cord, respectively. A bi-exponential was fit to the signal attenuation and PDFs were computed from the analytical Fourier transform. The height (PZERO), full width at half maximum (FWHM), root mean square displacement (RMSD), and kurtosis excess (KE, the deviation from Gaussian diffusion [7]) of the PDF were computed for each voxel. For conventional analysis, the perpendicular ($D_\perp$) and parallel ($D_\parallel$) diffusion constants, fractional anisotropy (FA) and mean diffusivity (MD) were computed by fitting the Stejskal-Tanner equation to the signal at low b-values ($\leq$ 2061 s/mm^2) assuming an oriented cylindrically symmetric tensor. A region of interest (ROI) analysis was done in the dorsal column to compare lesioned and contralateral WM. Histology was done on two additional rats (MRI data not shown) including luxol fast blue (LFB) for myelin and SMI-31 for phosphorylated neurofilaments (indicative of healthy axons).

Results and Discussion: Fig 1. At the level of L1, LFB staining shows no change in myelin pallor at 3 days, but decreased detection of SMI-31 suggests axonal damage. At 30 days, LFB shows visible loss of myelin staining while SMI-31 shows the persistence of axonal damage on the lesioned side. **Fig 2.** In DWIs at 30 days, a hypo-intensity on the lesioned side suggests a reduction in the barriers to perpendicular diffusion, whereas a hyper-intensity suggests an increase in barriers to parallel diffusion. Compared to contralateral WM, the PDF of perpendicular diffusion on the lesioned side is lower and broader (decreased $PZERO_\perp$ and increased $RMSD_\perp$), whereas the PDF of parallel diffusion is taller and narrower (increased $PZERO_\parallel$ and decreased $RMSD_\parallel$). **Fig 3.** The lesion is readily apparent on the diffusion contrast maps (selected shown). **Table 1** summarizes the percent change in diffusion contrasts between time points and contralateral WM. ***Perpendicular Diffusion:*** At 3 days, the increase in $D_\perp$ (36%) and $RMSD_\perp$ (18%) suggests that the loss of structural barriers (other than myelin), plays an important role for perpendicular diffusion. From 3 to 30 days, $D_\perp$ and $RMSD_\perp$ (18% to 57%) increased further, which may be related to the clearance of myelin during this period. The decrease in $KE_\perp$ shows that perpendicular diffusion is more Gaussian in the lesion (KE = 0 for Gaussian PDF). ***Parallel Diffusion:*** At 3 days, a decrease in $D_\parallel$ (39%) and $RMSD_\parallel$ (19%) agrees with histological findings of axonal injury. From 3 to 30 days, $D_\parallel$ was relatively unchanged, while $PZERO_\parallel$ increased and $FWHM_\parallel$ decreased, which could be due to q-space's sensitivity to changes in the slow diffusion component. Notably, the increase in $KE_\parallel$ shows that parallel diffusion is more restricted on the lesioned side, in line with the expectation of axonal "beading" and bulb formation in this animal model [1,8].

Conclusion: Our results suggest that early axonal degeneration and the gradual clearance of myelin can be detected with DWI. Whereas increased perpendicular diffusion was not specific to myelin damage, decreased parallel diffusion may be a specific marker for axonal damage. Furthermore, q-space analysis may provide a more comprehensive assessment of WM damage and offers several advantages over conventional DWI analysis including the measurement of KE and the quantification of the slow diffusion component at high b-values.

Fig 1. Histology of Dorsal Column

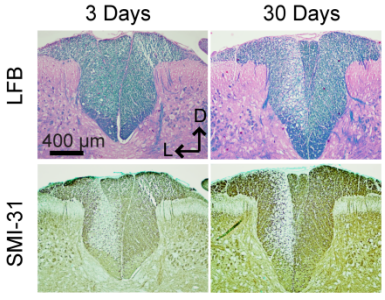

Fig 2. DWIs and Single Voxel PDFs

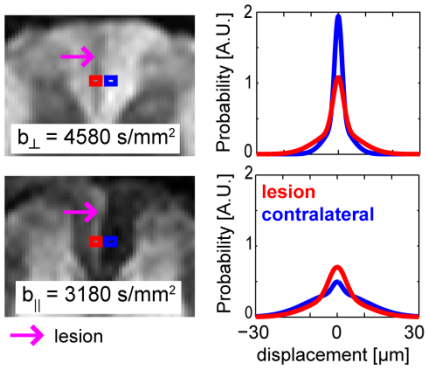

Fig 3. Selected Q-Space Diffusion Contrasts

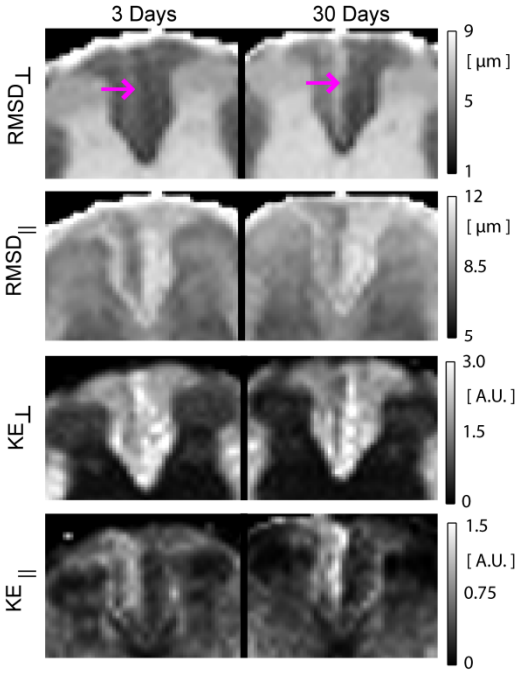

ROI-based Analysis: Percent Change of Diffusion Contrasts at 3 and 30 Days

Contrast	3 Days vs. Contralateral	30 Days vs. Contralateral	30 Days vs. 3 Days
$D_\perp$	36 ± 11	114 ± 13	65 ± 13
$D_\parallel$	-39 ± 7	-39 ± 3	4 ± 9
FA	-22 ± 4	-45 ± 5	-30 ± 8
MD	-23 ± 6	-8 ± 2	26 ±8
$PZERO_\perp$	-17 ± 3	-32 ± 6	-20 ± 5
$FWHM_\perp$	13 ± 4	24 ± 7	10 ± 5
$RMSD_\perp$	18 ± 5	57 ± 6	37 ± 6
$KE_\perp$	-27 ± 7	-39 ± 11	-20 ± 6
$PZERO_\parallel$	23 ± 10	42 ± 5	10 ± 7
$FWHM_\parallel$	-22 ± 16	-43 ± 4	-21 ± 7
$RMSD_\parallel$	-19 ± 3	-16 ± 1	5 ± 4
$KE_\parallel$	154 ± 57	261 ± 40	27 ± 17

References:
[1] George R, Griffin J.W., J Neurocytol 1994, 23:657.
[2] Cory D., Garroway A., MRM 1990, 14:435.
[3] Cohen Y., Assaf Y., NMR Biomed 2002, 15:516
[4] Assaf Y., et al, MRM 2000, 44:713. [5] Biton I.E., et al, MRI 2006; 24:161. [6] Nossin-Manor R., et al, MRI 2002, 20:231. [7] Latt J., et al, MRI 2008, 26:77
[8] Kerschensteiner M, et al, Nat. Med., 2005, 11(5):572.

Funding: NIH/NCRR-P41RR15241; NMSS CA1029A2,TR3760A3; NIH AG20012; Nancy Davis Center Without Walls